LETTERS

In situ multi-satellite detection of coherent vortices as a manifestation of Alfvénic turbulence

David Sundkvist[1,2], Vladimir Krasnoselskikh[1], Padma K. Shukla[3], Andris Vaivads[2], Mats André[2], Stephan Buchert[2] & Henri Rème[4]

Turbulence in fluids[1] and plasmas[2–5] is a ubiquitous phenomenon driven by a variety of sources—currents, sheared flows, gradients in density and temperature, and so on. Turbulence involves fluctuations of physical properties on many different scales, which interact nonlinearly to produce self-organized structures in the form of vortices[2–5]. Vortex motion in fluids and magnetized plasmas is typically governed by nonlinear equations[2–5], examples of which include the Navier–Stokes equation[1,2], the Charney–Hasegawa–Mima equations[2–5] and their numerous generalizations[6–9]. These nonlinear equations admit solutions[2–5] in the form of different types of vortices that are frequently observed in a variety of contexts: in atmospheres, in oceans and planetary systems[2,4], in the heliosphere[10,11], in the Earth's ionosphere and magnetosphere[12–17], and in laboratory plasma experiments[18]. Here we report the discovery by the Cluster satellites[19] of a distinct class of vortex motion—short-scale drift-kinetic Alfvén (DKA) vortices[8,9]—in the Earth's magnetospheric cusp region. As is the case for the larger Kelvin–Helmholtz vortices observed previously[17], these dynamic structures should provide a channel for transporting plasma particles and energy through the magnetospheric boundary layers.

The DKA vortices are result of nonlinear interaction of coupled finite-amplitude, low-frequency (in comparison with the proton gyrofrequency) drift and kinetic Alfvén waves[20], which accompany density, potential and sheared magnetic field perturbations, and which are propagating obliquely to the external magnetic field and density gradient directions. We present clear evidence that the DKA vortex structures exist on several spatial scales, contrasting them to those Alfvénic structures that have been deduced from simple magnetohydrodynamic (MHD) models[2,11]. The observed DKA vortices have a characteristic scale of the order of the ion (sound) gyroradius, $\rho_p \approx 25$ km. Hence, the electromagnetic DKA vortices, as discovered here, are in sharp contrast to a recent observation[17] of Kelvin–Helmholtz (KH) vortices which are typically 40,000 km across in space. Both the DKA and KH vortices provide new channels for transporting plasma particles and energy through the magnetospheric boundary layers, but on different spatio-temporal scales. Furthermore, it should be stressed that the DKA vortices are of fundamental interest also in the heliosphere[11] and in fusion plasmas[18] with regard to cross-field transport processes.

The formation of vortices is generally attributed to inverse cascade[1–5] of energy between two or three-dimensional (3D) dispersive modes that are nonlinearly interacting. For the DKA vortices in a non-uniform magnetoplasma, nonlinear equations[8,9] governing their dynamics include the evolution of nonlinearly coupled density perturbations, the ion vorticity, and the parallel (with respect to the external magnetic field direction) component of the vector potential. Owing to anisotropic dispersion characteristics of the DKA waves in a non-uniform magnetoplasma (with the plasma β—the ratio kinetic pressure/magnetic pressure—being larger than the electron-to-proton mass ratio), the above mentioned nonlinear equations admit inverse cascade, but the energy spectrum in the inertial range may not follow a Kolmogorov-like power law[1] because the turbulence now contains the characteristic scale ρ_p. This makes a clear distinction between the nonlinear dispersive DKA mode related vortices and those localized Alfvénic structures that are based on the nonlinear MHD equations[2,11]. Although extensive theoretical work has been carried out to investigate the properties of the DKA vortices[8,9,13], there are no direct microscale observations of these coherent structures in magnetized space plasmas. Earlier space-borne observations, which suggested vortex-like structures[13–16] in the Earth's ionosphere and magnetosphere, suffered from the inherent problem of separating temporal from spatial variations owing to limitations of single point measurements in space. Hence, up to now, the existence of the DKA vortices and many theoretical predictions regarding their properties could not be experimentally verified—for example, the characteristic length scale perpendicular to the ambient magnetic field direction, which is a crucial parameter for identifying the size of a plasma vortex.

The Cluster multi-spacecraft mission, with *in situ* simultaneous multi-point measurements[19], provides a unique opportunity to investigate the existence of the DKA vortices inside the cusp region of the Earth's magnetosphere, where there exist sheared plasma flows and density gradients sufficient to excite finite amplitude DKA fluctuations in a non-uniform magnetoplasma with $\beta \approx 0.02$. In the following, we present multipoint microscale measurements that unambiguously show the existence of short scale DKA vortices.

The cusp is an important region in the Earth's magnetosphere where the solar wind can directly access the ionosphere, and where large amounts of the plasma as well as kinetic and electromagnetic energies are transported. The cusp often exhibits the characteristics of low-frequency electromagnetic turbulence[16,21]. On 9 March 2002, the Cluster satellites passed outward through the high-altitude northern cusp during a time of northward interplanetary magnetic field[21]. Under such conditions, high-latitude magnetic reconnection takes place tailward from the cusp. A turbulent boundary layer on the border between the cusp and the polar cap is then formed, characterized by reconnection induced field-aligned proton jets. The four Cluster satellites entered the region of the turbulent boundary layer at 02:49 UT (Fig. 1). The cusp is identified as a high-density region with the presence of intense ion flux (Fig. 2a, b). Associated with these proton injections, there are broadband low-frequency electromagnetic fluctuations of Alfvénic nature ($E_\perp/B_\perp \approx v_A$, where $\perp$ denotes perpendicular components and v_A is the Alfvén speed) around and below the proton gyrofrequency, $f_{cp} \approx 1.6$ Hz, giving rise to the turbulent spectra shown in Fig. 2c (only the magnetic

[1]Laboratoire de Physique et Chimie de l'Environnement, CNRS, 45071 Orléans, France. [2]Swedish Institute of Space Physics, SE-751 21 Uppsala, Sweden. [3]Institut für Theoretische Physik IV, Ruhr-Universität Bochum, D-44780 Bochum, Germany. [4]Centre d'Etude Spatiale des Rayonnements, Toulouse 31029, France.

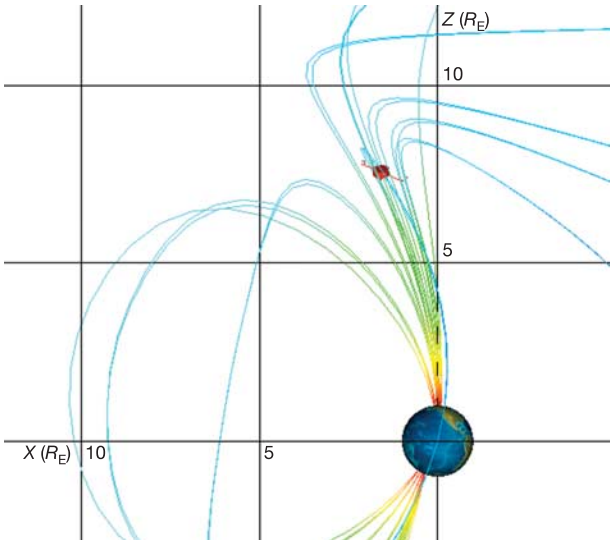

Figure 1 | Location of the Cluster spacecraft and the Earth's magnetic field lines. The red line marks the trajectory of the spacecraft for the time interval in Fig. 2, while traversing outbound through a boundary layer to the cusp. The interplanetary magnetic field was northward and reconnection occurred on the same field lines at higher altitudes. R_E, Earth radius.

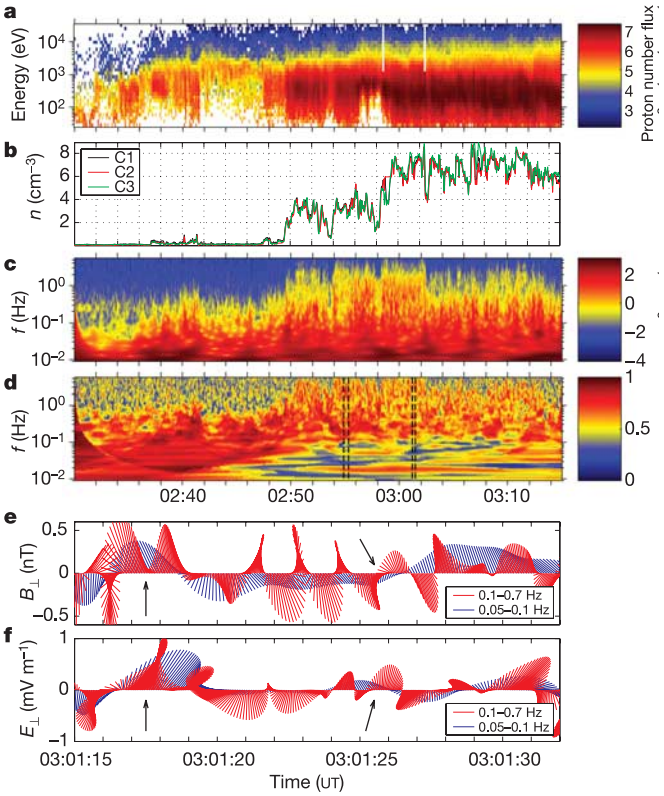

Figure 2 | Proton flux, density and low frequency fields for a cusp passage. **a**, Proton number flux. **b**, Plasma density, n, measured by three of the Cluster spacecraft, C1, C2 and C3. **c**, Power spectral density of magnetic field strength B as a function of frequency f and time. A wavelet transform has been used to better resolve the low-frequency structures. **d**, Degree of polarization (DOP) of the three components of the magnetic field, which can be viewed as a test for plane waves. Note how the DOP decreases dramatically for emissions below ~0.1–0.2 Hz when entering the boundary layer to the cusp, implicitly indicating the presence of structures. **e**, Hodogram representations of perpendicular magnetic field, $B_\perp$, for two frequency intervals, corresponding to different spatial scales through a Doppler shift. The arrows shows where rotational reversal occurs. **f**, Same as **e**, here for the perpendicular electric field.

spectrogram is shown here). The Alfvén speed is typically around 1,000 km s^{-1} in this region. Direct multi-point measurements[21] revealed the presence of coupled drift and kinetic Alfvén waves (KAWs) as well as electromagnetic ion-cyclotron waves whose characteristic perpendicular scale-lengths are of the order of (2–4)ρ_p. The boundary layer plasma is strongly inhomogeneous (density gradients up to 25% at distances of a few proton gyroradii), with prevalent shear velocity flows[21]. These gradients are well above the theoretical threshold values for spontaneously exciting finite amplitude DKA waves which self-organize in the form of vortical structures. Below, we study the low-frequency electromagnetic waves in detail, and show that a significant part of the frequency spectrum can be attributed to coherent DKA vortex structures.

The result of a polarization analysis of the three magnetic field components in the frequency domain around and below the proton gyrofrequency is displayed in Fig. 2d. The degree of polarization[22] (DOP) can be regarded as a test for the plane wave ansatz. A high value of DOP implies that the fluctuations considered as linear plane waves are coherent over several wavelengths. The sudden drop in DOP at frequencies below 0.1–0.2 Hz, when the spacecraft enters the cusp boundary layer, indicates that the electromagnetic field fluctuations can be structures, rather than plane wavepackets. Hodogram representations of the perpendicular magnetic and electric fields along the spacecraft trajectory (Fig. 2e, f) indeed show rotation reversal behaviour reminiscent of vortices. Moreover, we notice that the vortex structures exist nested on several different scales (Fig. 2e, f). To demonstrate that the observed variations are coherent vortex structures, it is necessary to show their characteristics and their spatial origin. The latter was not possible with earlier single-spacecraft measurements. We now demonstrate the spatial occurrence of these structures by using the fact that we have four simultaneous measurement points in space.

Figure 3e exhibits the configuration of the Cluster spacecraft in the plane perpendicular to the ambient magnetic field direction, together with the projection of the convective plasma flow velocity $V_\perp$ at about 02:55 UT on 9 March 2002. The relative velocity between the spacecraft and the bulk plasma is ~28 km s^{-1}. The relative alignment of the C1 and C2 spacecrafts along the plasma flow vector (Fig. 3e) predicts that a structure fixed in the plasma frame should be visible on both spacecraft with a time lag of approximately one second. Moreover, a quasi-static structure of the size of a few ρ_p will be Doppler-shifted in frequency domain to $f \approx V_\perp/\lambda_\perp \approx 0.1$–0.3 Hz, where $\lambda_\perp$ is the typical perpendicular scale size. The time series of the perpendicular magnetic field components, which are bandpass filtered at 0.1–0.2 Hz, are depicted in Fig. 3a, b. The time lag between the spacecraft is clearly visible and is about 1.2 s, which is consistent with the spacecraft observing a quasi-stationary structure moving with the plasma flow. Observations by the C3 and C4 satellites, which are not aligned along the flow with any other satellites, do not correlate with the observations from other spacecraft (Fig. 3d, e), thus giving an estimate of the transverse radial scale size of the structure of the order of (2–3)ρ_p.

To confirm the vortex nature of the coherent structures, we perform an analysis of the temporal evolution of the instantaneous direction of the magnetic field vectors (Fig. 3c, d). The angle between the magnetic field and the fixed direction of the spacecraft trajectory shows the polarization reversal feature, which is a unique characteristic of a vortex: polarization change on its spatial scale. At 02:55:03 UT and 02:55:16 UT (indicated by arrows) the sense of rotation changes direction from left-handed to right-handed and then back again.

We have demonstrated that the variations are spatially coherent vortex structures. Taken together with their Alfvénic nature in a strongly inhomogeneous magnetoplasma, we conclude that we have

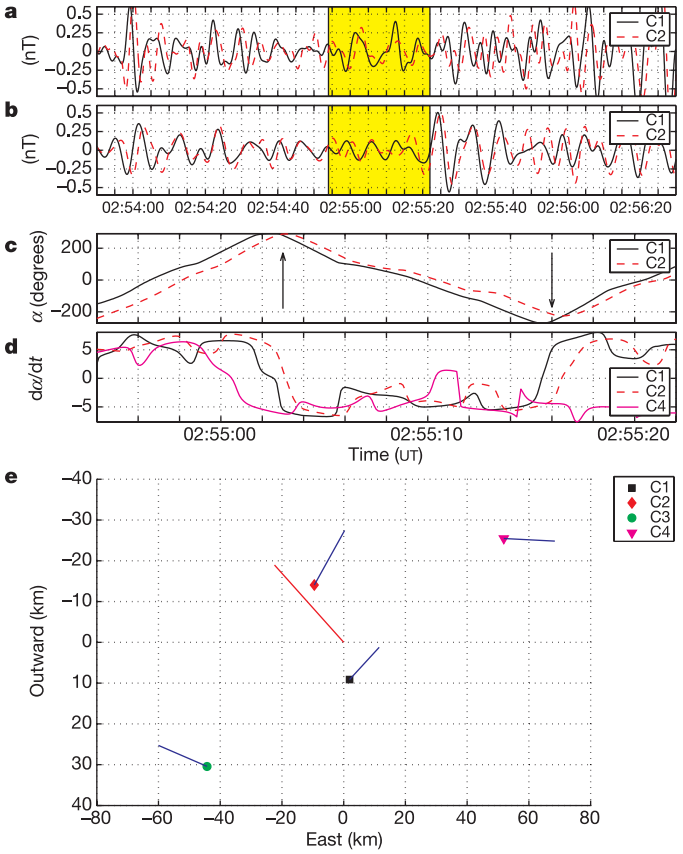

Figure 3 | Magnetic field data from the Cluster satellites. The time series are filtered to correspond to the length scales of the Doppler shifted structures. **a**, Eastward perpendicular component of the magnetic field. The highlighted area is used for panels **c** and **d**. **b**, Similarly, the outward perpendicular component. **c**, Angle α between the instantaneous magnetic field vector in the perpendicular plane and a fixed direction in this plane, corresponding to the highlighted area in **a** and **b**. It should be pointed out that the sense of rotation changes direction from left-handed to right-handed and then back again during this time interval. **d**, Angular velocity of the same angle as in **c**. **e**, Relative positions of the satellites in the plane perpendicular to the ambient magnetic field. The plasma flow vector was mainly in this plane and is shown by the red line. The length of the vector indicates the distance the plasma convects with respect to the satellites during one second. The blue lines represent the instantaneous magnetic field measured on board respective spacecraft. Note that C1 and C2 are almost exactly aligned along the flow vector.

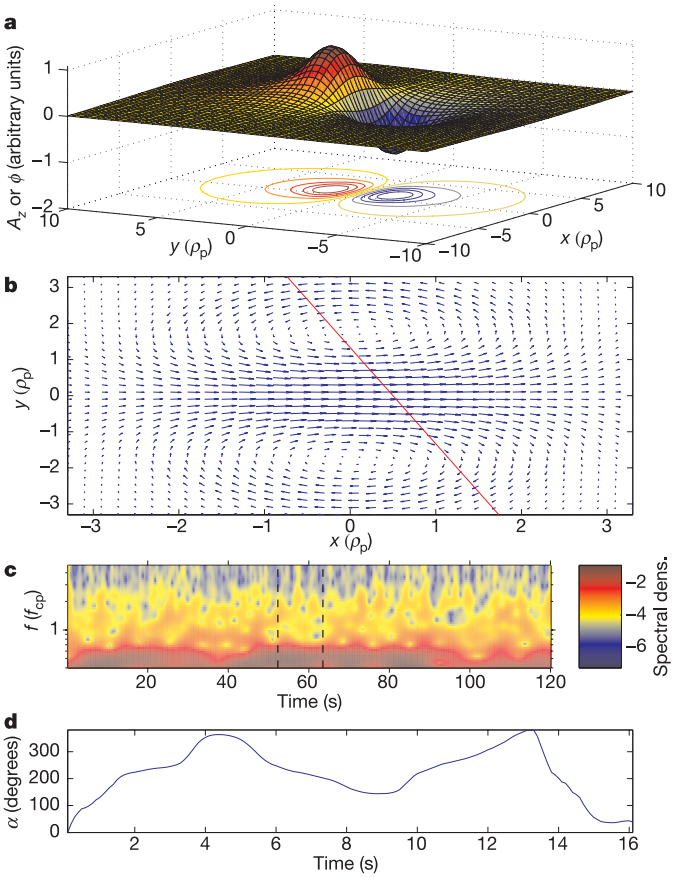

Figure 4 | Analytical DKA vortex solution and a vortex model for the turbulence in the cusp. **a**, Magnetic vector potential A_z or scalar potential Φ of a dipole Alfvénic vortex. **b**, Magnetic field in perpendicular plane calculated from A_z. Note the rotation of the field vectors. The red line is an example of a spacecraft trajectory through the vortex field. **c**, Magnetic field spectral intensity from a model time series for Alfvénic turbulence consisting of a series of vortices in the plasma. Compare with Fig. 2c. **d**, the angle α between instantaneous perpendicular magnetic field and a simulated spacecraft trajectory through the model field for the time period marked with vertical lines in **c**. Compare with Fig. 3c.

indeed observed short scale coherent DKA vortices. The angular rotation in Fig. 3c, d is consistent with a vortex chain convected past the spacecraft. We can also estimate the characteristic size of the DKA vortex from these time series. It is difficult to say when one vortex ends and the next begins, but we note (Fig. 3c, d) that the typical time period is of the order of 10–20 s, which corresponds to spatial radial scales of the order of $(3–6)\rho_p$. Thus, we have two independent methods for calculating the transverse spatial scale that are in agreement with each other—one from the spatial configuration of the spacecraft at the same instant of time, and the other from the time series as the vortices are convected past the spacecraft. This is also in good agreement with the theoretical estimate[8,9], which gives the radial scale-size as $\sim 3\rho_p$. The vortices propagate along (across) the geomagnetic field lines with a speed comparable to the Alfvén speed, v_A ($(0.01–0.1)v_A$).

Strong electromagnetic wave turbulence in a non-uniform magnetoplasma can be considered as an ensemble of nonlinear dispersive Alfvén and drift-waves, DKA vortices, and quasi-magnetostatic structures[23]. We have constructed an isolated DKA vortex model[8,9] for conditions applicable to the cusp plasma, and used it to extract the main characteristic features to be compared with our observational data (Fig. 4). An example of the magnetic field from such a model is shown in Fig. 4c. The spectrogram has been obtained from simulating a spacecraft trajectory through a model field, the temporal fluctuations depending solely upon a Doppler shift of quasi-static DKA vortices (compare Fig. 4b). The spectra obtained are broadband with the largest intensities in the lowest frequencies, and can be compared to the observed field in Fig. 2c. The angular rotation of the magnetic field, while passing through a vortex chain (Fig. 4d), is in perfect agreement with our observations (Fig. 3c).

Received 15 March; accepted 16 June 2005.

1. Frisch, U. *Turbulence: The Legacy of A.N. Kolmogorov* (Cambridge Univ. Press, Cambridge, 1995).
2. Petviashvili, V. I. & Pokhotelov, O. A. *Solitary Waves in Plasmas and in the Atmosphere* (Gordon and Breach Science Publishers, Philadelphia, 1992).
3. Horton, W. & Hasegawa, A. Quasi-two-dimensional dynamics of plasmas and fluids. *Chaos* **4**, 227–251 (1994).
4. Pokhotelov, O. A., Stenflo, L. & Shukla, P. K. Nonlinear structures in the earth's magnetosphere and atmosphere. *Plasma Phys. Rep.* **22**, 852–863 (1996).
5. Horton, W. Drift waves and transport. *Rev. Mod. Phys.* **71**, 735–778 (1999).
6. Shukla, P. K., Yu, M. Y. & Varma, R. K. Formation of kinetic Alfvén vortices. *Phys. Lett. A* **109**, 322–324 (1985).
7. Petviashvili, V. I. & Pokhotelov, O. A. Dipole Alfvén vortices. *JETP Lett.* **42**, 54–56 (1985).

8. Shukla, P. K., Yu, M. Y. & Stenflo, L. Electromagnetic drift vortices. *Phys. Rev. A* **34,** 3478–3480 (1986).
9. Liu, J. & Horton, W. The intrinsic electromagnetic solitary vortices in magnetized plasma. *J. Plasma Phys.* **36,** 1–24 (1986).
10. Burlaga, L. F. A heliospheric vortex street. *J. Geophys. Res.* **95,** 4333–4336 (1990).
11. Zhou, Y., Matthaeus, W. H. & Dmitruk, P. Magnetohydrodynamic turbulence and time scales in astrophysical and space plasmas. *Rev. Mod. Phys.* **76,** 1015–1035 (2004).
12. Hones, E. W. *et al.* Further determination of the characteristics of magnetospheric plasma vortices with ISEE 1 and 2. *J. Geophys. Res.* **86,** 814–820 (1981).
13. Chmyrev, V. M. *et al.* Alfvén vortices and related phenomena in the ionosphere and the magnetosphere. *Physica Scripta* **38,** 841–854 (1988).
14. Chmyrev, V. M. *et al.* Vortex structures in the ionosphere and magnetosphere of the earth. *Planet. Space Sci.* **39,** 1025–1030 (1991).
15. Stasiewicz, K. *et al.* Small scale Alfvénic structure in the aurora. *Space Sci. Rev.* **92,** 423–533 (2000).
16. Savin, S. *et al.* Turbulent boundary layer at the border of geomagnetic trap. *JETP Lett.* **74,** 547–551 (2001).
17. Hasegawa, H. *et al.* Transport of solar wind into Earth's magnetosphere through rolled-up Kelvin-Helmholtz vortices. *Nature* **430,** 755–758 (2004).
18. Spolaore, M. *et al.* Vortex-induced diffusivity in reversed field pinch plasmas. *Phys. Rev. Lett.* **93,** 215003 (2004).
19. Escoubet, C. P., Schmidt, R. & Goldstein, M. L. Cluster—science and mission overview. *Space Sci. Rev.* **79,** 11–32 (1997).
20. Weiland, J. *Collective Modes in Inhomogeneous Plasma* (IoP Publishing, Bristol, 2000).
21. Sundkvist, D. *et al.* Multi-spacecraft determination of wave characteristics near the proton gyrofrequency in high-altitude cusp. *Ann. Geophys.* **23,** 983–995 (2005).
22. Samson, J. C. Some comments on the descriptions of the polarization states of waves. *Geophys. J. R. Astr. Soc* **61,** 115–129 (1980).
23. Volokitin, A. S. & Dubinin, E. M. The turbulence of Alfvén waves in the polar magnetosphere of the earth. *Planet. Space Sci.* **37,** 761–765 (1989).

Acknowledgements The authors thank the FGM, EFW and CIS Cluster instrument teams for supplying data for this study. Gratitude goes to T. D. de Wit for his help with the wavelet calculations. The research of D.S., V.K. and P.K.S. was partially supported by the European Commission. The research of A.V. was supported by the Swedish Research Council.

Author Information Reprints and permissions information is available at npg.nature.com/reprintsandpermissions. The authors declare no competing financial interests. Correspondence and requests for materials should be addressed to D.S. (davids@irfu.se).

ERRATUM

doi:10.1038/nature04144

In situ multi-satellite detection of coherent vortices as a manifestation of Alfvénic turbulence

David Sundkvist, Vladimir Krasnoselskikh, Padma K. Shukla, Andris Vaivads, Mats André, Stephan Buchert & Henri Rème

Nature 436, 825–828 (2005)

In the print and PDF versions of this Letter, the colour scale bars in Fig. 2a, c and d should have been respectively labelled as follows: 'Proton number flux ($cm^{-2}\,s^{-1}\,sr^{-1}\,keV^{-1}$)'; '$B$ ($nT^2\,Hz^{-1}$)'; and 'DOP'. This labelling is correctly shown in the online HTML full text version.

ERRATUM

doi:10.1038/nature04145

Evasion of intracellular host defence by hepatitis C virus

Michael Gale Jr & Eileen M. Foy

Nature 436, 939–945 (2005)

In Table 1 of this Review Article, some reference citations are incorrect. Those in the fourth row from the top (IRF-1 regulation) should be 89,90 (and not 93,94); in the second-to-last row from top (regulation of RIG-I signalling), reference 94 should be included (to read 21,94).

CORRIGENDUM

doi:10.1038/nature04146

Action potential refractory period in ureter smooth muscle is set by Ca sparks and BK channels

T. Burdyga & Susan Wray

Nature 436, 559–562 (2005)

The panels of Fig. 3 in this Letter are incorrectly cited in the text. In the first full paragraph on page 560, these should be: line 7, 'Fig. 3b, top'; line 11, 'Fig. 3b'; line 12, 'Fig, 3c, top'; and line 13, 'Fig. 3c, bottom'. Other citations of Fig. 3 are correct. In addition, the vertical voltage scale on the bottom trace in Fig. 3d should read from −70 to 10 mV.